Research Article

GRNN Prediction Model for Temperature-Induced Deformation of CRTS II Unballasted Slab Track

Kitisak Kanjanun, Yan Bin and Yao Shuang'ao
Department of Railway Engineering, School of Civil Engineering, Central South University, Changsha, Hunan, China

Sakda Katawaethwarag*
Department of Teacher Training in Civil Engineering, Faculty of Technical Education, King Mongkut's University of Technology North Bangkok, Bangkok, Thailand

* Corresponding author. E-mail: sakda.k@fte.kmutnb.ac.th DOI: 10.14416/j.asep.2021.12.003
Received: 9 October 2021; Revised: 22 November 2021; Accepted: 25 November 2021; Published online: 16 December 2021

Abstract
The General Regression Neural Network (GRNN) is one of the algorithms of Artificial Neural Networks (ANN) that receives much attention in prediction applications. This research used the GRNN to predict the temperature-induced deformation of unballasted track structures based on experimental data considering external weather conditions, such as sunshine duration, rain conditions, daily maximum temperature, daily minimum temperature, and daily average wind speed. The GRNN network predicts the average absolute error of the prediction results (0.0318 ℃), the maximum absolute error (1.7729 ℃), and the GRNN prediction sample mean squared error (0.070701). The average relative error is 0.32%. The finding of this study shows that the GRNN prediction method has good accuracy and robustness. Furthermore, it can promote the research of unballasted track temperature fields that are related to concrete structures.

Keywords: Track engineering, Temperature-induced deformation, The artificial neural network, GRNN algorithm

1 Introduction

1.1 *The CRTS-II unballasted*

The CRTS-II unballasted slab track has been widely used in China. It has been modified from the Bögl unballasted track system, the German continuous welded rail system [1], [2]. The problems of unballasted slab track, produced by a prestressed concrete slab, have the factors with the effect on the structure or environmental loads, such as vibrational, noise, meteorology utilizing temperature, rain, snow, wind, solar radiation, and increase construction prices causing continual influence degradation of unballasted slab track properties [3]–[5]. However, heat transfer in the temperature exchange is absorbed and exhaled by solar radiation steadily directly or reflected transfer energy from high-temperature area to low-temperature area. Figure 1 shows a heat transfer mechanism regarding to an unballasted slab track [5], [6]. When the temperature load action on around surface of the unballasted slab track in distribution forms a nonlinear thermal conducting expansion with stress and strain and causes flexural deformation slab track structure due to a temperature load [3], [7], [8]. The significant influence to design the unballasted slab track is the temperature load [9]. The ambient air temperature convection is a natural environmental source that affects temperature variations over the concrete slab track section depth and width. The experimental field study observed the temperature gradient in the unballasted track structure [3]. Temperature-induced deformation brought a significant consideration in the unballasted track [3]. Many researchers have a focused observation on the

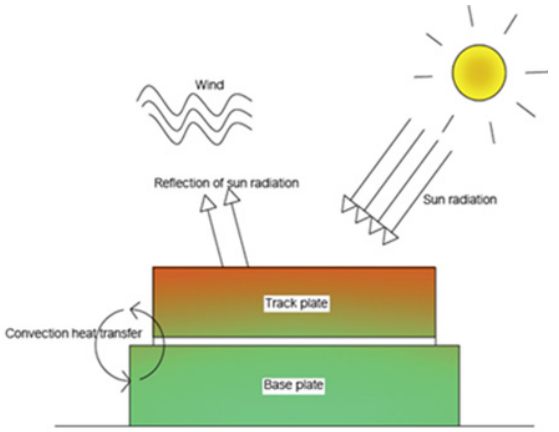

Figure 1: Mechanism of heat transfer unballasted slab track.

behavior of concrete slab tracks due to temperature change producing a mechanical process by performing experiments on a sample and then by comparing it with a mathematical model to determine the statistical factor causing the transformation processes leading to deformation. Based on the experiment, most factors resulted from temperature load mode when considering the temperature gradient within the axial force, therefore, the temperature load affects the track structure's stability and smoothness. The track damage can directly threaten the safety of train operations.

1.2 *The artificial neural network (ANN)*

The artificial neural network (ANN) is a system that mimics the human brain's processing [10]. ANN becomes a new essential step due to AI (Artificial Intelligence) development with functions that can understand and learn a range of knowledge, such as awareness, learning, reasoning, and solving problems. With these capabilities used, AI is now using in almost every industries, from the marketing level to the supply chain, finance, and food processing. Compared to other aspects of applying to machine learning and deep learning algorithms, AI applications must use the ANN model, as shown in Figure 2, like how the nervous system works in the human brain. These networks have 'Neurons' that connect to the 'nervous system' and communication. They use parallel processing to understand and learn from the big data that is continually received from sources. The algorithms

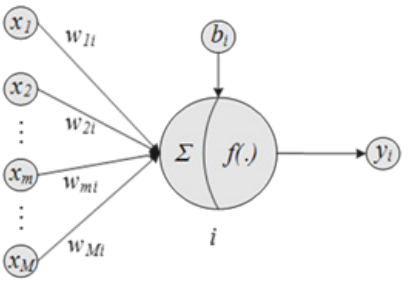

Figure 2: Artificial neuron model.

used to learn from the example and experience based on the principles that everything has a pattern indicating the possibility of that thing to and implement this pattern. It can be applied to predict the prospects, for example, using machine learning to predict sun radiation's effect in an unballasted track from the past and the present data. Therefore, as mentioned above, ANN combines artificial intelligence procession with a nonlinear numerical, such as logic, mathematical statistics, neural computing, and emblematic. Using algorithms can create a mathematical model to replace mathematical calculations and legal complexity and to increase predictions' efficiency under enormous data with fewer error values. As a result of this ANN, the property makes it very suitable for predictive use due to data accuracy [10].

1.3 *General regression neural network (GRNN)*

GRNN is an alternative algorithm to predict statistical, mathematical nonlinear structures with high parallelism. Although, there is scattered information in the measurement area, many dimensions, but the algorithm provides a smooth transition from one observed value to another. The algorithm used a pattern for any regression. In contrast, the algorithm makes regression where the target variable is continuous. Moreover, many researchers have proposed the GRNN algorithm as a more suitable algorithm than FFNN, CFNN, and ELMNN [10]–[13]. Because there are determination processes that are advantages over regression modeling, uncomplicated techniques applied in the relationships between the input and output assimilated are variables into the connection weights of the network [12], [14]–[19]. Therefore, they can fit to complex nonlinear

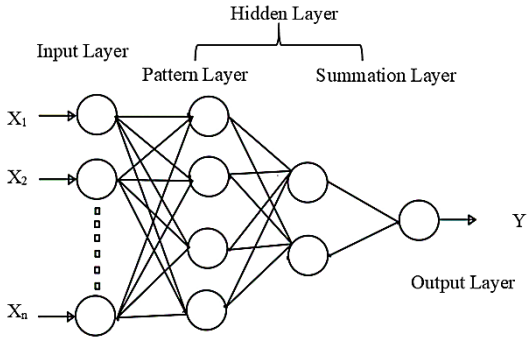

Figure 3: GRNN model.

models, but not specified in advance and several predictive function stages in making models. About advantage in choosing the prediction simulation model algorithm with the GRNN algorithm (Figure 3), it is modeled based on time series and temperature probability of estimating the expected data analysis in field experiment data to predict accuracy. Therefore, it is essential that these studies focused on the effect of the temperature resulting in the CRTS II Unballasted slab track's deformation by observation, collection of meteorological data, and data analysis techniques for time series to create an intelligent model [17], [20].

2 Materials and Methods

Unballasted track temperature field experiment, continuous observation field experiment of temperature on CRTS II unballasted slab track for four months on the passenger was dedicated. The geographical coordinates of the observation site are 28°N and 115°E by Central South University. The sampling tool is a temperature sensor embedded in the joints of the unballasted track structure, as shown in Figure 4(a). The collecting temperature gradient data at time interval is half an hour in 5 observation points A, B, C, D, E, and the observation positions correspond to 4 cm, 12 cm from the surface of the track plate, 4, 14, and 32 cm from the base plate's surface as shown in Figure 4(b) [4], [21]–[24]. During the observation period, the number of sunshine hours in this area is 0~10.7 h. The daily average wind speed is 0.6~5.6 m/s, the daily minimum temperature is –5~25 ℃, and the daily maximum temperature is 5~35 ℃. The sunny and rainy weather is cross-distributed. All these data are shown in Figure 5.

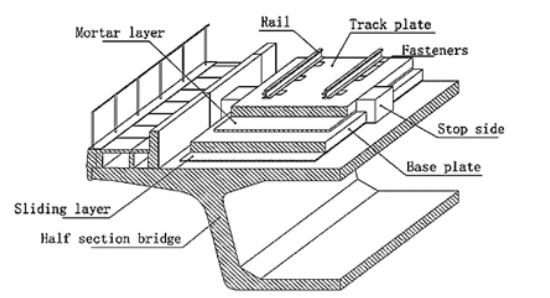

(a)

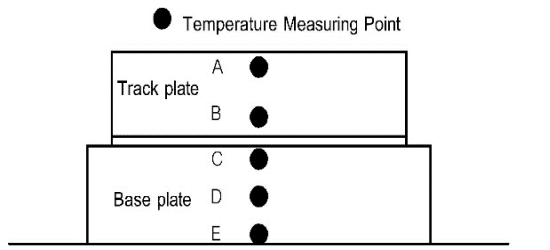

(b)

Figure 4: (a) CRTS II unballasted slab track configuration, (b) Location of the temperature sensor.

3 GRNN Modeling Prediction

GRNN Modeling Prediction due to the experimental data is a nonlinear relationship [25]. Therefore, it is more complicated to directly characterize the regression relationship in the generalized regression neural network. The input layer's function identifies input variables and passes the input vector to the pattern layer, as shown in Figure 6 [15], [16], [26]. The number of neurons in this layer is an equation to the input vector's dimension [11]. The number of neuron nodes in the pattern layer equals the number of neuron nodes in the input layer, equal to the input sample's dimension. The expression of the transfer function is as follows Equation (1):

$$q_i = \exp\left[\frac{(X - X_i)^T (X - X_i)}{2\delta^2}\right], \; i = 1, 2, \ldots, n \tag{1}$$

The hidden layer needs to perform two types of summation on the data passed down by the pattern layer Equations (2) and (3). It is precise because of two types of summation: in explaining the generalized regression neural network principle, the final output

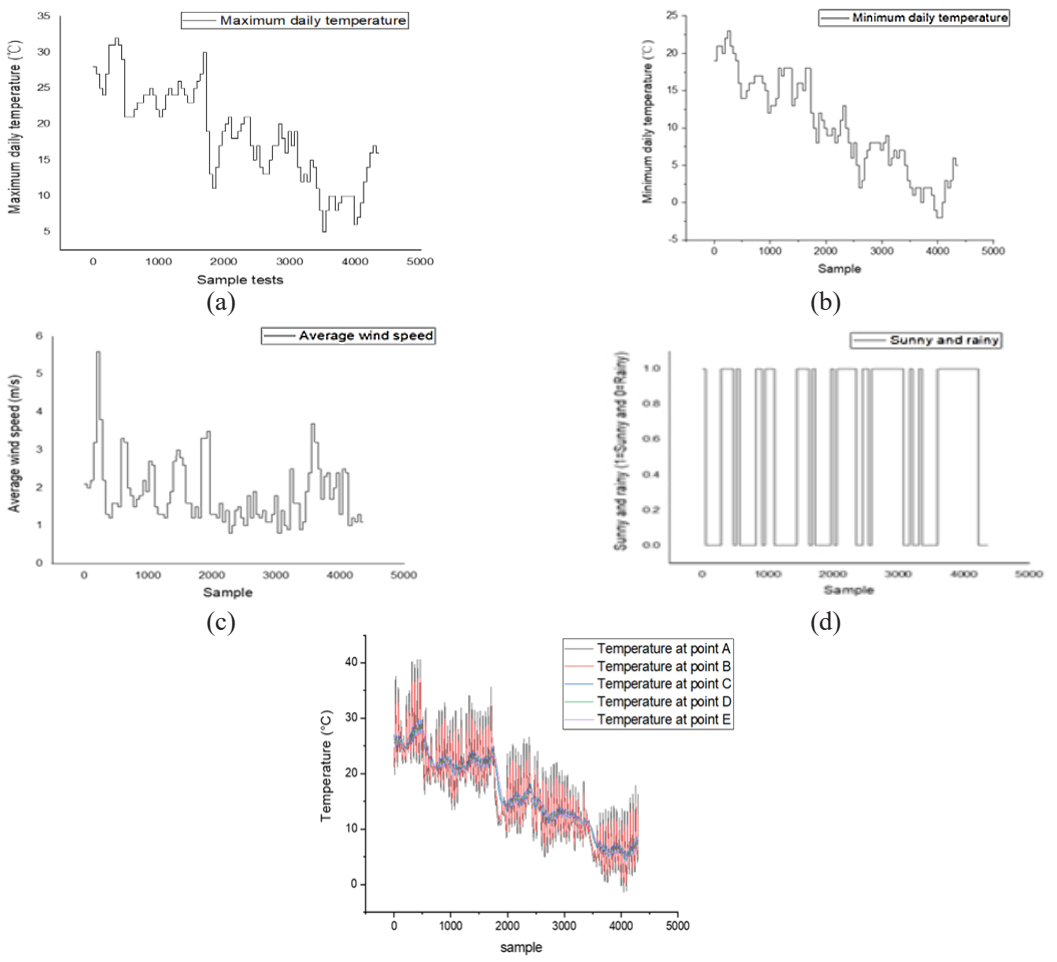

Figure 5: (a) Maximum daily temperature, (b) lowest daily temperature, (c) Daily average wind speed, (d) Daily sun radiation, and (e) Comparing temperature distribution.

estimate is part of the prior probability described in Equation (4).

$$s_1 = \sum_{i=1}^{n} q_i \tag{2}$$

$$s_1 = \sum_{i=1}^{n} Y_i q_i = \sum_{i=1}^{n} Y_i q_i, j \tag{3}$$

$$y_j = \frac{S_{2j}}{S_1}, j = 1, 2, \ldots, k \tag{4}$$

The basic principle of generalized regression neural network is to find the y value corresponding to the maximum probability. The input vector X is the relevant basis for network calculation and evaluation; the initial condition for obtaining Y's predicted value is the input vector X.

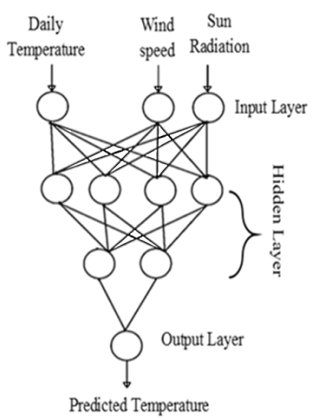

Figure 6: GRNN Prediction model.

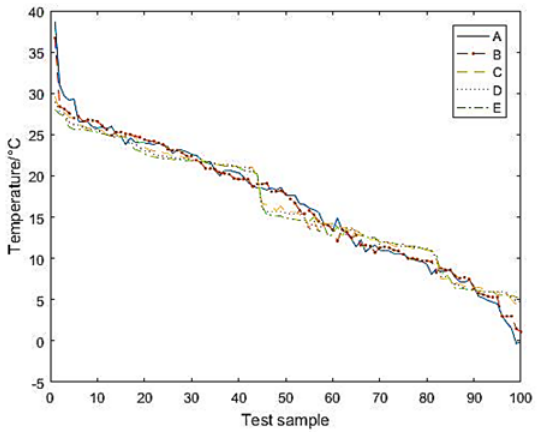

Figure 7: The actual distribution of temperature at the measuring points of the test set.

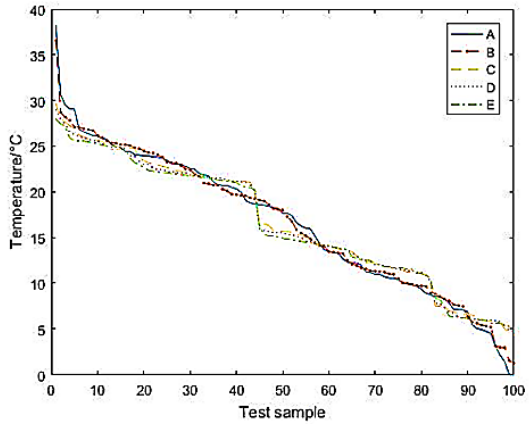

Figure 8: GRNN prediction result of the temperature distribution of the test set samples.

The expression of the predicted value Y in output value Y where f (X, Y) is the joint density distribution function of random variables X, Y. is as follows:

$$\hat{Y} = E(Y|X) = \frac{\int_{-\infty}^{\infty}(X, y)dy}{\int_{-\infty}^{\infty}(X, y)dy} \quad (5)$$

The selected variable within the measurement data time establishes the neural network, daily maximum temperature, daily minimum temperature, sunny, and daily average wind speed. Sunshine duration is an independent variable, an input parameter.

4 Results and Discussion

4.1 *The experimental data*

Figure 7 depicts the distribution of the experimental temperature data of the field experiment on points A, B, C, D, and E by selecting 100 dataset that was randomly selected from 4100 observation data. Figure 8 represents the GRNN prediction model based on the data within the regression analysis on points A, B, C, D, and E in 100 sets of output test data. The prediction results' average absolute error is 0.0318 ℃, the maximum absolute error is 1.7729 ℃, and the GRNN prediction sample mean squared error is 0.070701. The average relative error is 0.32%. The most distributed errors are between –0.5 and 0.5 ℃, as shown in Figure 9. These are the error between the actual temperature distribution at the measuring points

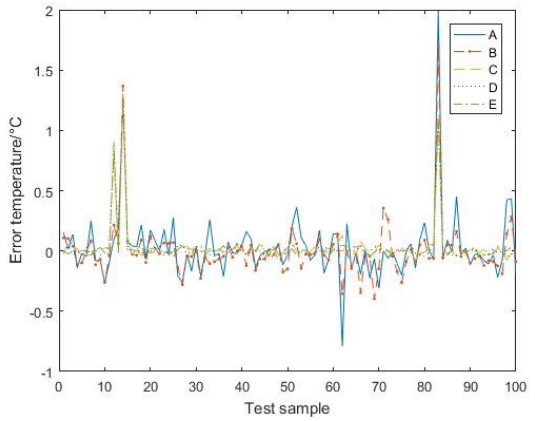

Figure 9: The distribution of prediction errors of the test set samples.

of the test set (Figure 7) and GRNN predicting results (Figure 8). There are specific differences in each measuring point's prediction errors due to the different measurement errors and temperature changes. Based on the above GRNN model with the data analysis, the temperature gradient of the ballastless track structure in this area is summarized and analyzed. There is an apparent nonlinear relationship in the temperature of the ballastless track. Figure 10 shows the field experimentation elicited through experiment untraining data compared with the GRNN model elicited through training data that shows each error by randomly selected. It can be seen that GRNN has more minor error data than field experimentation. There is also

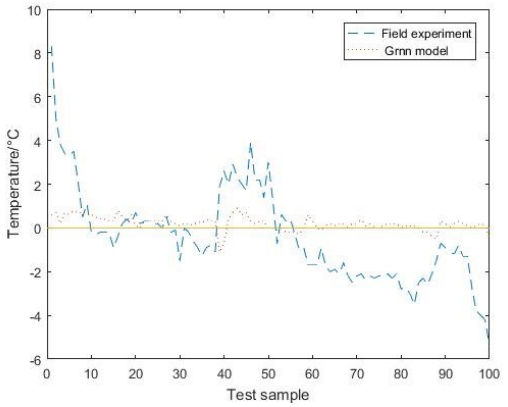

Figure 10: Comparison of the untrained field experimented error and GRNN model error.

an error value that is narrower and more precise. The GRNN model method can obtain the better data analysis than the traditional testing method.

4.2 *Performance of GRNN prediction model*

The GRNN shows that the prediction results of the GRNN model, the maximum absolute error is 1.327 °C. The concentrated errors are between –0.5 and 0.5 °C, which all errors are within a reasonable range compared with a randomly divided up the 100 target timesteps by cross-validated with a data set of 70% for learning, 15% for model validation, and 15% for model testing with problem definition y(t) = f(x(t–1), x(t–d). Performance of the GRNN Prediction Model (Figures 11–14) shows the regression R-values of the training, validation, and test data were 0.7836, 0.77906, 0.76786, and 0.74324, respectively [20]. The histogram shows the frequency distribution of prediction errors of GRNN using data sets between training, cross-validation, and test represented in Figure 15. It can be seen that the data behavioral in the prediction model have linear regressions correlated to the output of the model, and this confirms the reliability of the model based on GRNN.

5 Temperature-Induced Deformation

Temperature-induced deformation from the thermal expansion theory, the temperature coefficient of concrete expansion is more diminutive than steel in the region of 15–20 °C and even higher around 100 °C [3],

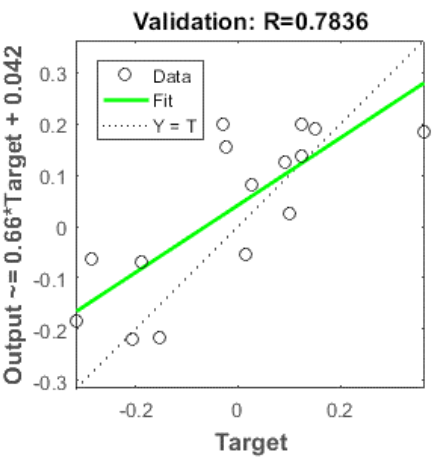

Figure 11: Result of random sample in the network.

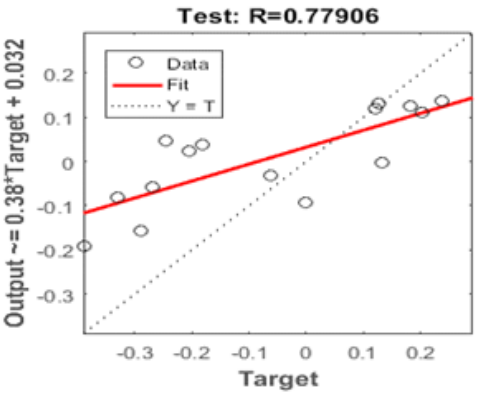

Figure 12: Regression result from training data.

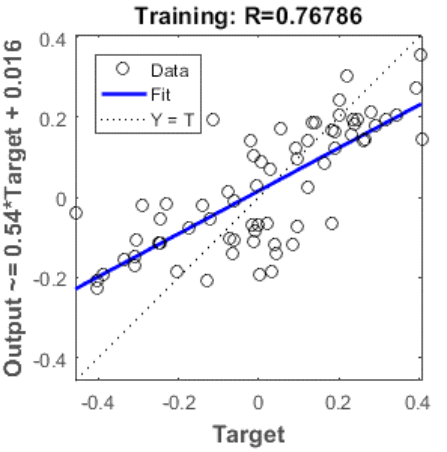

Figure 13: Regression result from test data.

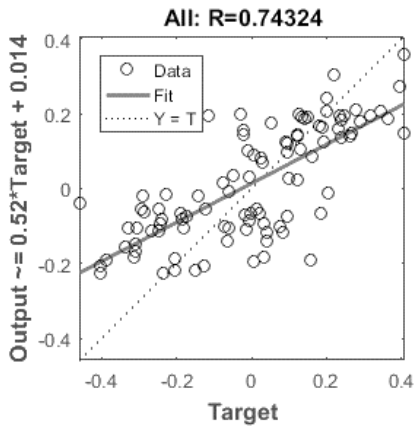

Figure 14: Regression result from all data.

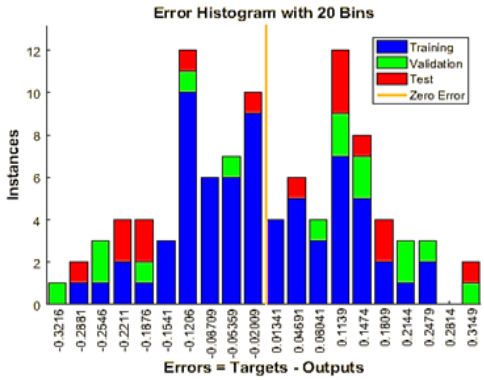

Figure 15: The histogram of the prediction error distribution.

[23], [27]. If concrete is heated rapidly, the structure expands, corresponding to a more considerable value of the temperature changing makes expansion and shrinkage reduction [23], [27]. Due to the slow heat transfer of concrete, each temperature value of the lower structure of the unballasted track usually corresponds to two temperature load distribution states. One is that the surface of the track slab has a significant degree of heat transfer, and the temperature of the corresponding position shows different degrees. On the other hand, the state where the degree of heat dissipation on the track surface is large and the corresponding position's heat dissipation rate was the cause of difference of the unballasted track in this area concentrated are between –5 °C and 5 °C. The unballasted track section was separated into two parts, the base plate, and the track plate. Because of the isolation layers, when the temperature increases, the less-flexible structures layer can slip of structural parts and increase the internal stress to be the cause of deformation in that section. After a structure changes its shape, it can lead to structural cracking if the temperature gradient increases. In this research, the overall influence of the temperature deformation difference on deflection and deformation of the unballasted track is in a controllable range. The GRNN prediction model, based on the network model itself, can perform qualitative analysis on the ballastless track's meteorological parameters.

6 Conclusions

Based on the temperature field experiment's data analysis, the prediction results' average absolute error is 0.0318 °C, and the maximum absolute error is 1.7729 °C. The GRNN prediction sample mean squared error is 0.070701, and the average relative error is 0.32%. The GRNN Prediction Model's performance, shown in the training's regression R-values, was 0.7836, 0.77906, 0.76786, and 0.74324, respectively indicates that the training was accurately correlated. The network model's error and the measurement data's limitations show a correlation coefficient that the training was accurately correlated. The degree of influence on the temperature field action mode is different degrees of cross-influencing factors among the influencing factors are converted effectively. The meteorological factors' effective conversion is to realize various factors' indicators and quantify the meteorological factors. This study found that the GRNN prediction method has good accuracy. Temperature-induced deformation in the unballasted track in this area concentrated are small has changed the overall influence of the temperature deformation effect on the deflection and deformation of the unballasted track is within a controllable range. Based on the GRNN prediction model, ambient temperature can be used to calculate the data to predict the emergence of temperature-induced deformation in the unballasted track. It can be seen that the GRNN model method is more effective than the full-scale traditional testing methodology. It economizes the cost, time, and labor of testing as an alternative method for testing in artificial intelligence (AI) for railway engineering in the 21st century.

Acknowledgments

The authors gratefully thank the School of Civil Engineering, Central South University, for fund support.

References

[1] Y. Bin, G. Dai, and N. Hu, "Recent development of design and construction of short span high-speed railway bridges in China," *Engineering Structures*, vol. 100, pp. 707–717, Oct. 2015.

[2] R. Bastin, "Development of German non-ballasted track forms," in *Proceeding of the Institution of Civil Engineer-transport*, vol. 159, no. 1, pp. 25–39, Feb. 2006.

[3] X. Song, C. Zhao, and X. Zhu, "Temperature-induced deformation of CRTS II slab track and its effect on track dynamical properties," *Science China Technological Sciences*, vol. 57, no. 10, pp. 1917–1924, Oct. 2014.

[4] H. Xiao, Y. Zhang, Q.-h. Li, F. Jin, and N. Mahantesh, "Analysis of the initiation and propagation of fatigue cracks in the CRTS II slab track inter-layer using FE-SAFE and XFEM," *Proceedings of the Institution of Mechanical Engineers, Part F: Journal of Rail and Rapid Transit*, vol. 233, no. 7, pp. 678–690, Aug. 2019.

[5] Y. Zhong, L. Gao, P. Wang, and S. J. Liang, "Mechanism of interfacial shear failure between CRTSII slab and ca mortar under temperature loading," *Gongcheng Lixue/Engineering Mechanics*, vol. 35, no. 2, pp. 230–238, Feb. 2018.

[6] L. Zhou, Y. Yuan, L. Zhao, A. D. G. Mahunon, L. Zou, and W. Hou, "Laboratory investigation of the temperature-dependent mechanical properties of a CRTS-II ballastless track-bridge structural system in summer," *Applied Sciences*, vol. 10, no.16, Aug. 2020, Art. no. 5504.

[7] Y. Bin, G. Dai, and H. T. Su, "A meteorological parameters-based prediction model of vertical temperature gradient of track plate," *Huanan Ligong Daxue Xuebao/Journal of South China University of Technology (Natural Science)*, vol. 42, no. 12, pp. 9–13, Dec. 2014.

[8] R. Yang, J. Li, W. Kang, X. Liu, and S. Cao, "Temperature characteristics analysis of the ballastless track under continuous hot weather," *Journal of Transportation Engineering, Part A: Systems*, vol. 143, no. 9, Sep. 2017, Art. no. 04017048.

[9] G. Dia, H. T. Su, Y. Bin, and J. P. Zhu, "Nonlinear temperature distribution of longitudinal plate-type ballastless track in spring," *Journal of South China University of Technology (Natural Science Edition)*, vol. 44, no. 2, pp. 20–25, Feb. 2016.

[10] T. Khatib, A. Mohamed, K. Sopian, and M. Mahmoud, "Assessment of artificial neural networks for hourly solar radiation prediction," *International Journal of Photoenergy*, vol. 2012, Jun. 2012, Art. no. 946890.

[11] D. F. Specht, "A general regression neural network," *IEEE Transactions on Neural Networks*, vol. 2, no. 6, pp. 568–576, Nov. 1991.

[12] Z. Juan and Y. Kaiyun, "General regression neural network forecasting model based on PSO algorithm in water demand," in *2010 Third International Symposium on Knowledge Acquisition and Modeling*, 2010, pp. 51–54.

[13] M. Martinez-Blanco, G. Ornelas-Vargas, L. Solis-Sánchez, R. Castañeda-Miranada, H. Vega-Carrillo, J. C. Padilla, I. Garza-Veloz, M. L. Martinez-Fierro, and J. M. Ortiz-Rodriguez, "A comparison of back propagation and generalized regression neural networks performance in neutron spectrometry," *Applied Radiation and Isotopes*, vol. 117, pp. 20–26, Nov. 2016.

[14] N. Ceryan, U. Okkan, and A. Kesimal, "Application of generalized regression neural networks in predicting the unconfined compressive strength of carbonate rocks," *Rock Mechanics and Rock Engineering*, vol. 45, no. 6, pp. 1055–1072, Nov. 2012.

[15] H. Cigizoglu, "Generalized regression neural network in monthly flow forecasting," *Civil Engineering and Environmental Systems*, vol. 22, no. 2, pp. 71–81, Jun. 2005.

[16] H. K. Cigizoglu and M. Alp, "Generalized regression neural network in modelling river sediment yield," *Advances in Engineering Software*, vol. 37, no. 2, pp. 63–68, Feb. 2006.

[17] H. Zhao and S. Guo, "Annual energy consumption forecasting based on PSOCA-GRNN model," *Abstract and Applied Analysis*, vol. 2014, Aug. 2014, Art. no. 217630.

[18] Z. Alizadeh, J. Yazdi, J. H. Kim, and A. K. Al-Shamiri, "Assessment of machine learning

techniques for monthly flow prediction," *Water*, vol.10, no. 11, Nov. 2018, Art. no. 1676.

[19] A. O. Ratip, A. W. Okoth, and R. Wanyonyi, "A generalized regression neural network model for maize production in Trans Nzoia County," *International Journal of Mathematics Trends and Technology (IJMTT)*, vol. 65, no.10, pp. 54–60, Oct. 2019.

[20] S. Lee, S. Jung, and J. Lee, "Prediction model based on an artificial neural network for user-based building energy consumption in South Korea," *Energies*, vol. 12, no. 4, Feb. 2019, Art. no. 608.

[21] O. Zumin and L. Fujian, "Analysis and prediction of the temperature field based on in-situ measured temperature for CRTS-II ballastless track," *Energy Procedia*, vol. 61, pp. 1290–1293, 2014.

[22] H. Su, Y. Bin, and G. Dai, "Temperature filed experimental study of longitudinally connected ballastless track on bridge in one year period," *IABSE Symposium Report*, vol. 106, no. 8, pp. 580–589, May 2016.

[23] Z. W. Li, X. Z. Liu, and Y.-L. He, "Identification of temperature-induced deformation for HSR slab track using track geometry measurement data," *Sensors*, vol. 19, no. 24, Dec. 2019, Art. no. 5446.

[24] G. Dai, H. T. Su, and Y. Bin, "Experimental study on the vertical temperature gradient of longitudinally connected slab ballastless track on bridge in autumn," *Hunan Daxue Xuebao/ Journal of Hunan University (Natural Sciences)*, vol. 42, no. 3, pp. 94–99, Mar. 2015.

[25] K. Kerbouche, S. Haddad, A. Rabhi, A. Mellit, M. Hassan, and A. E. Hajjaji, "A GRNN based algorithm for output power prediction of a PV panel," in *Artificial Intelligence in Renewable Energetic Systems*. Cham, Switzerland: Springer, 2018.

[26] H. K. Cigizoglu, "Artificial neural networks in water resources," in *Integration of Information for Environmental Security*. Dordrecht, Netherlands: Springer, 2008, pp. 115–148.

[27] E. Freyssinet, "The deformation of concrete," *Magazine of Concrete Research*, vol. 3, no. 8, pp. 49–56, Dec. 1951.